

Elstob Alison, Uday Patel, and Michael Gonsalves

Abbreviations

CT	Computed tomography
CECT	Contrast-enhanced CT
CEUS	Contrast-enhanced ultrasound
DWI	Diffusion-weighted imaging
FSE	Fast spin echo
FDG	Fluorine-18 fluoro-2-deoxyglucose
GRE	Gradient-recalled echo
PET	Positron emission tomography
RCC	Renal cell carcinomas
US	Ultrasound

Key Messages

- Incidental detection of small renal masses is increasingly common, and these masses require accurate characterisation with imaging to facilitate management decisions.
- Contrast-enhanced CT (CECT) has high diagnostic accuracy for the diagnosis of RCC and remains the mainstay for radiological evaluation of both cystic and solid lesions.
- MRI and contrast-enhanced US are good techniques for problem-solving in lesions deemed indeterminate by CECT or for patients in which CECT is contraindicated.
- In a mass that demonstrates measurable enhancement on CT or MRI, no specific imaging features can conclusively distinguish between RCC and oncocytoma.
- Percutaneous biopsy should be considered in lesions that remain indeterminate after initial imaging investigations.

E. Alison • U. Patel • M. Gonsalves (✉)
St George's Hospital, London, UK
e-mail: Michael.Gonsalves@stgeorges.nhs.uk

3.1 Background

Over the last decade, the incidence of renal cancer in the United Kingdom has increased by almost a third [1]. This is largely attributable to

increased incidental detection, due to the widespread use of cross-sectional imaging. Currently, between 50 and 61% of all renal cancers are detected incidentally, compared with only 13% in the 1970s [2, 3]. There has been an associated stage migration with incidentally detected renal cell carcinomas (RCC) tending to be of both lower stage and grade. Optimum management of small renal tumours poses a particular challenge to the renal cancer multidisciplinary team, for two key reasons. Firstly, up to 20% of renal masses smaller than 4 cm in diameter are benign [4–6]. Secondly, there are multiple management strategies available to clinicians including nephrectomy, partial nephrectomy, ablation and observation. Accurate characterisation of renal masses is therefore fundamental to achieving the best outcomes for patient with small renal tumours. In this chapter, the different imaging modalities will be evaluated, and their role in characterising both small cystic and solid renal lesions will be discussed.

The Goals of Imaging: Key Questions to Be Answered

1. Is the mass solid or cystic?
2. Is the mass benign or malignant?
3. Does the tumour exhibit features of biological aggressiveness?
4. What anatomical information can be provided to aid surgical treatment and decision-making?

3.2 Computed Tomography

CT is the primary imaging modality used for identification and characterisation of small renal masses. In this section we will discuss the imaging features that enable differentiation between solid and cystic lesions and potentially between benign and malignant lesions. While these features are discussed in the context of CT imaging, they are applicable to other imaging modalities.

Accurate CT evaluation of a small renal mass can only be achieved with reference to the clinical history of the patient. The majority of inflammatory, vascular or post-traumatic “pseudotumours” can be diagnosed correctly when the clinical history highlights the possibility of these conditions (Fig. 3.1).

3.2.1 Enhancement

Enhancement of renal masses is considered to be the most important factor in distinguishing between a cyst and a solid renal mass [7, 8]. A renal mass protocol CT must therefore include images obtained before and after administration of iodinated contrast media. Post-contrast images should be obtained during the nephrographic phase (85–120 s post-contrast administration) as there is maximal and homogeneous enhancement of renal parenchymal, increasing the conspicuity

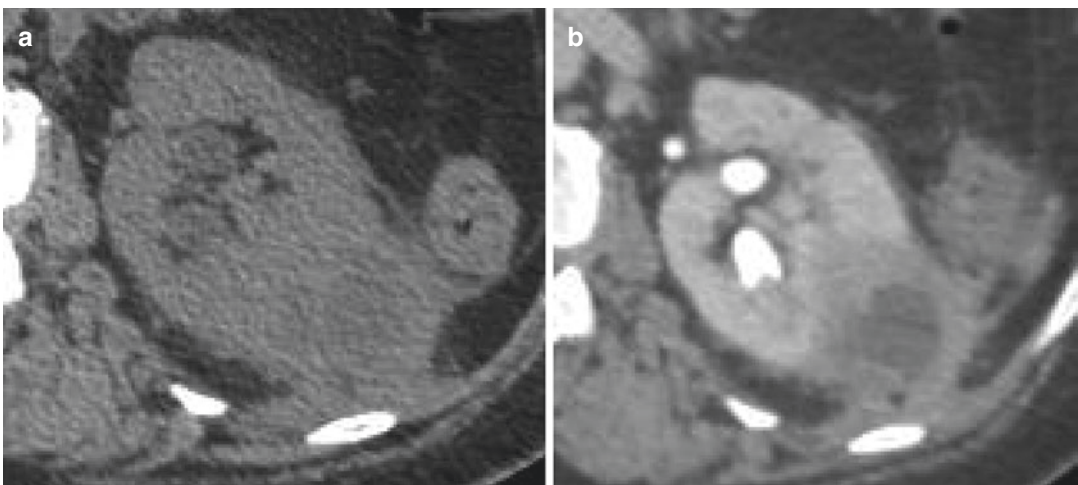


Fig. 3.1 Pre- (a) and (b) post-contrast axial CT images demonstrate a rim enhancing left interpolar lesion with adjacent perinephric stranding. Aspirated material cultured *E. coli*

of renal masses. An increase in the attenuation of a renal lesion of at least 20 Hounsfield units (HU), following contrast administration, represents definitive enhancement and is in keeping with a solid lesion or solid component [8]. A lesion with post-contrast enhancement of less than 10 HU is classed as non-enhancing. Lesions enhancing by 10–20 HU are considered to be indeterminate and will require further characterisation (Figs. 3.2, 3.3, 3.4 and 3.5).

The main limitation of the use of enhancement is lesion size. As lesion size decreases, sampling

error and image artefacts can lead to erroneous attenuation measurements and potential misclassification of renal lesions [8, 9]. Multiple authors have questioned the reliability of attenuation measurements in sub-centimetre masses.

3.2.2 Macroscopic Fat

Macroscopic fat within a solid renal lesion is highly suggestive of angiomyolipoma (AML), the commonest benign renal neoplasm. Macroscopic

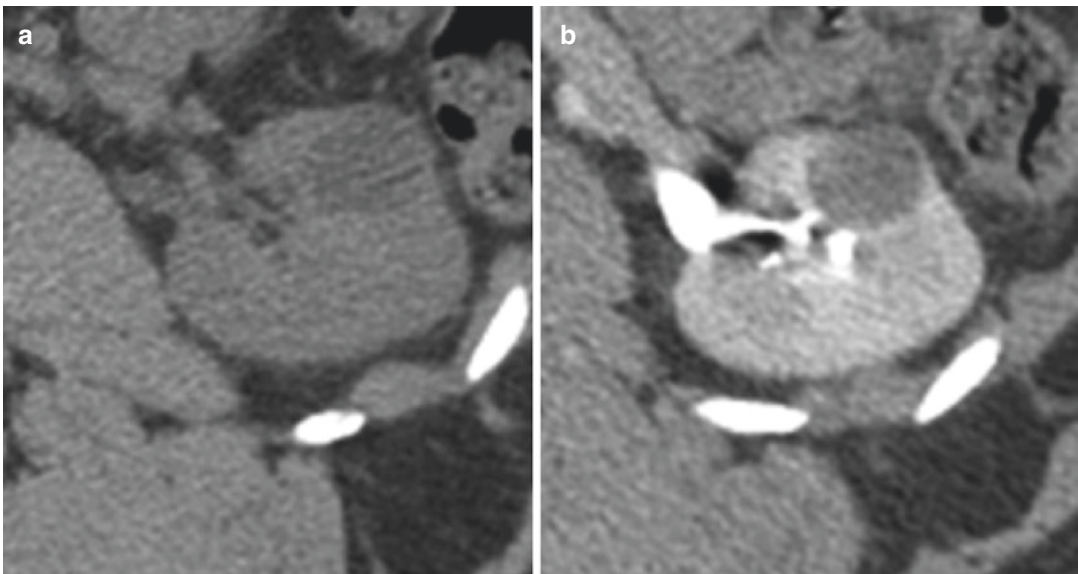


Fig. 3.2 Simple cyst. Pre- (a) and (b) post-contrast axial CT images demonstrate enhancement of less than 10 HU

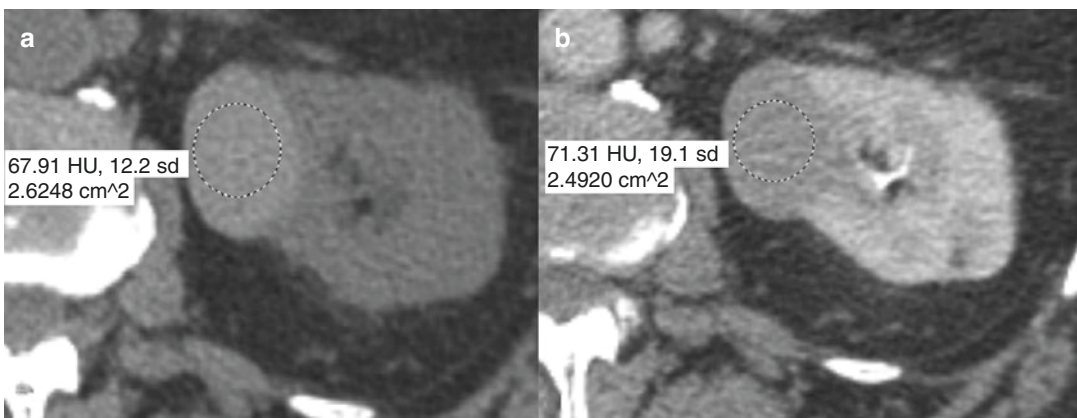


Fig. 3.3 Pre- (a) and (b) post-contrast axial CT images demonstrate indeterminate enhancement of 14 HU. This was confirmed as a hyperdense cyst on ultrasound

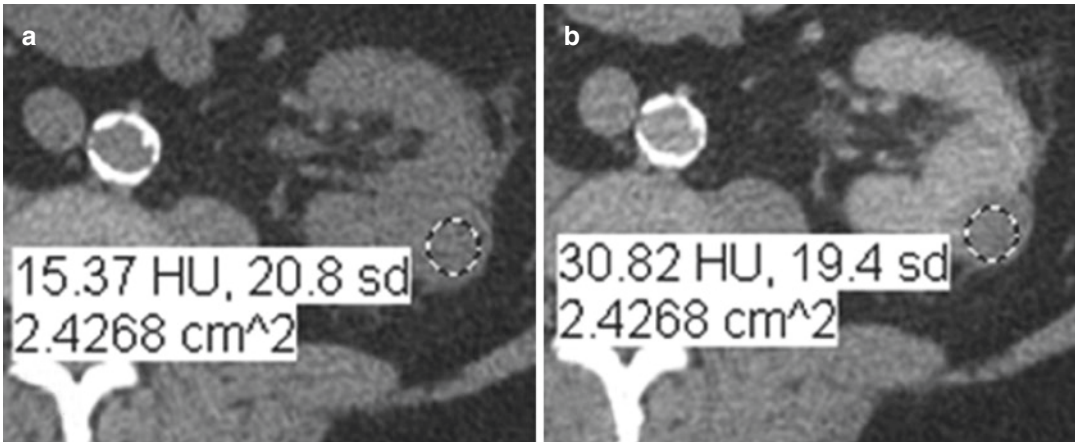


Fig. 3.4 Pre- (a) and (b) post-contrast axial CT images demonstrate indeterminate enhancement of 15 HU. Histology confirmed a papillary type 1 RCC

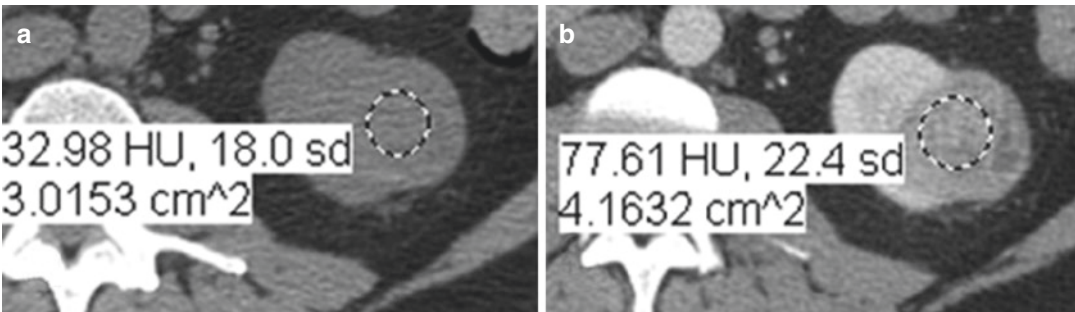


Fig. 3.5 Pre- (a) and (b) post-contrast axial CT images demonstrate post-contrast enhancement of 45 HU. Histology confirmed a clear cell RCC

fat is best demonstrated on unenhanced CT, where it returns characteristic low attenuation, measuring between -10 HU and -100 HU (Fig. 3.6).

AMLs are pathologically classified as choristomas, containing muscle, fat and vascular tissue. The relative proportions of these tissues vary between AMLs, but the majority of lesions are fat-rich, resulting in the classical imaging finding of macroscopic fat. 3–4.5% of AMLs contain microscopic fat not detectable by CT [10, 11] and can be misdiagnosed as RCC. Further diagnostic confusion can arise in the setting of RCCs containing macroscopic fat [12–15]. Various mechanisms have been described to explain the presence of intra-tumoural fat including engulfment of perinephric or renal sinus fat [14], osseous metaplasia

[12] and cholesterol necrosis [15]. A potential differentiator between fat-poor AML and fat-containing RCC is the presence of coexisting calcification [12], which occurs within fat-containing RCC but is extremely rare in AML (Figs. 3.7 and 3.8).

3.2.3 Growth Rate

Multiple studies have demonstrated growth rate to be of limited utility in distinguishing between benign and malignant renal masses. Small renal tumours grow slowly regardless of histopathological subtype with average growth rates reported to be 0.28 cm/year (range of 0.09–0.86 cm/year) [16]. 70% of small renal masses under imaging

surveillance will not exhibit measurable growth during follow-up periods of up to 32 months [17–20], and Kunkle et al. found that enhancing renal lesions that did not grow during a 24-month follow-up period were about as likely to be malig-



Fig. 3.6 Coronal post-contrast CT image demonstrates a right upper pole lesion containing macroscopic fat

nant (83%) as the lesions that did exhibit growth (89%) [20]. Several authors have reported no statistically significant difference in growth rates between small RCCs and oncocytomas [16, 21].

Fast growth rates during early follow-up within the first year are a potentially useful indicator of aggressive tumours. In a meta-analysis of 284 solid lesions, only 2% of patients developed metastases at a mean follow-up of 33.5 months. However, the mean growth rate of the metastatic group was double that of other lesions, at 0.8 cm/year [22] (Figs. 3.9 and 3.10).

3.2.4 Central Scar

Oncocytomas are the second commonest benign renal neoplasm, accounting for approximately 3–7% of all renal lesions [23]. The presence of a central stellate scar is often suggested as a feature of oncocytoma; however, this is not a reliable imaging finding. Less than half of all oncocytomas show a central scar [24] with some authors reporting this feature to be present in as few as 11% of cases [25]. Necrosis within RCC can lead to central areas of low attenuation mimicking a scar. There is currently no CT imaging feature that reliably distinguishes RCC from oncocytoma (Figs. 3.11 and 3.12).

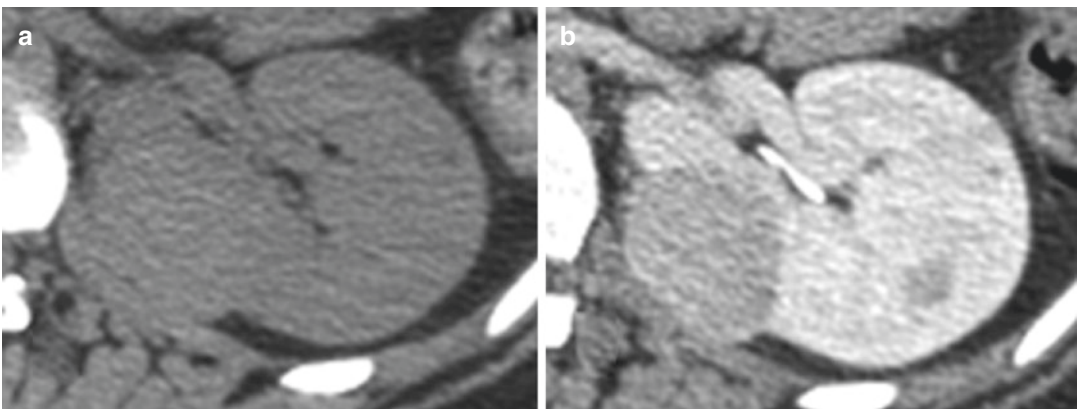


Fig. 3.7 Pre- (a) and (b) post-contrast axial CT images demonstrate an enhancing lesion with no visible macroscopic fat in a patient with tuberous sclerosis. Biopsy proven as an AML

3.3 CT of Small Cystic Renal Masses

Renal cysts are common, estimated to be present in 50% of adults over 50 years of age [26]. However, as 6% of asymptomatic renal masses have been shown to be cystic renal malignancies [27], a robust method for evaluating cystic renal masses is required. The Bosniak classification of renal cystic lesions was first described in 1986

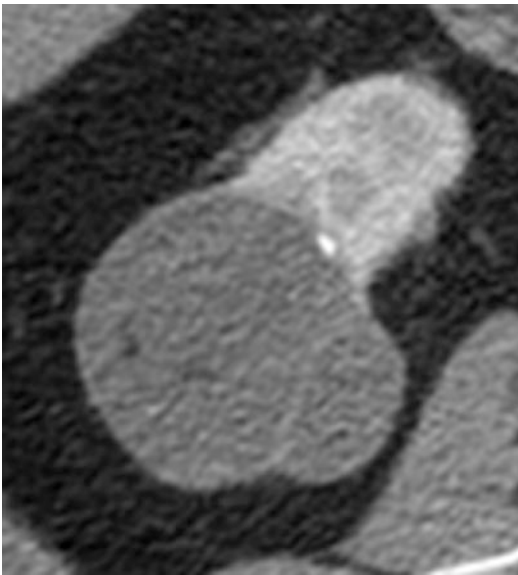


Fig. 3.8 Post-contrast axial CT image demonstrates an enhancing mass containing macroscopic fat and a small focus of peripheral calcification. Biopsy proven as a papillary RCC type 1

and has subsequently gained widespread acceptance [8, 28]. Bosniak described five categories of cystic renal mass ordered in increasing probability of malignancy (summarised in Table 3.1 and Fig. 3.4).

A series evaluating 116 cystic renal masses found good concordance between Bosniak classification and histopathology, with the authors concluding that Bosniak classification is useful for separating surgical from non-surgical cystic lesions [29]. High-quality CT is critically important in the accurate characterisation of cystic renal masses [29–31] (Fig. 3.13).

3.4 Morphometric Scoring Systems

In the last 5 years, several systems have been proposed to help evaluate the anatomical complexity of small renal masses. The main catalyst for these scoring systems has been shift in surgical practice towards treating a greater proportion of small renal masses with partial rather than radical nephrectomy. The R.E.N.A.L. nephrometry score and PADUA classification systems are the most widely used and are clearly outlined in their original articles [32, 33].

Other scoring systems have been described including the C index method that evaluates the single anatomical feature of proximity of tumour to the central renal sinus [34], renal tumour inva-

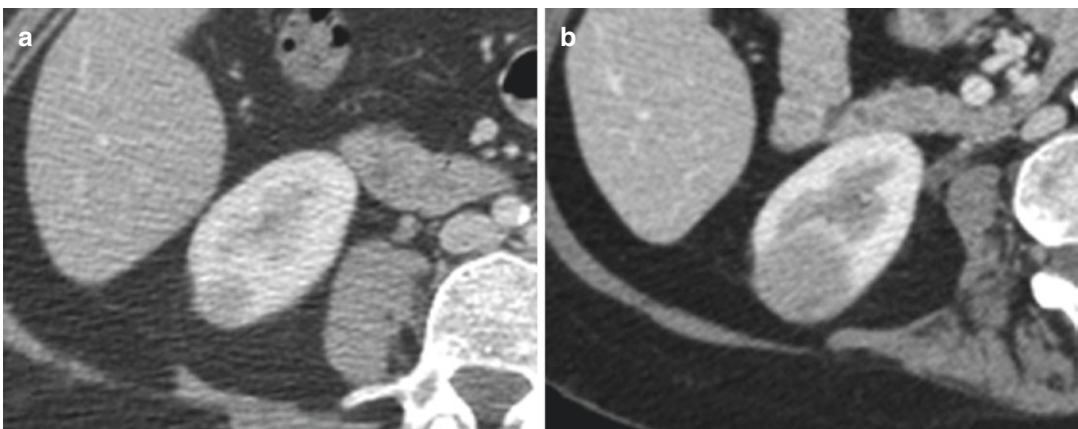


Fig. 3.9 (a, b) Post-contrast axial CT images of a clear cell RCC over a 5-year period showing typical slow growth



Fig. 3.10 Serial post-contrast axial CT images of renal mass in a patient with lung cancer, at baseline (a), at 3 months (b) and at 6 months (c). The mass demonstrated rapid growth. Biopsy proven as metastasis from the primary SCC of the lung



Fig. 3.11 Coronal post-contrast CT image of a left lower pole lesion with central scar. Histology confirmed this to be an oncocytoma

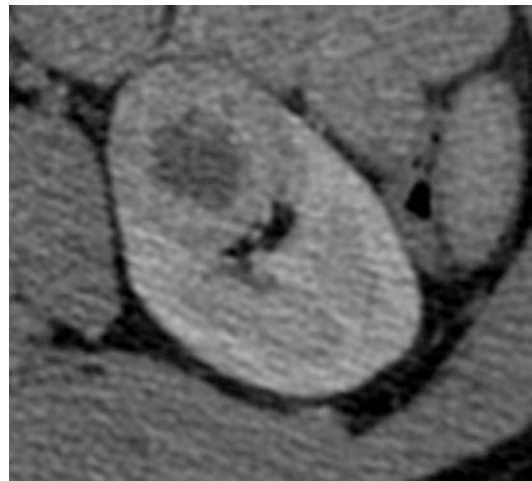


Fig. 3.12 Axial post-contrast CT image of an enhancing left renal mass with a central area of low attenuation which mimicked a scar. Histology proven to be a clear cell RCC

Table 3.1 Bosniak classification of renal cystic lesions (adapted from reference 8, Israel and Bosniak 2005)

Category	Imaging features	Management
I	Water attenuation, hairline thin wall with no septa, calcifications or solid components. No enhancement	No intervention Benign, simple
II	Few hairline thin septa that may enhance (not measurably). Fine calcification or short segment of thickened calcification in wall or septa Or uniformly high-attenuation lesion <3 cm that does not enhance	No intervention Benign
IIF	Multiple hairline thin septa, perceived (not measurable) enhancement of septa or wall Minimal thickening of septa or wall. Thick or nodular calcification in wall or septa Totally intrarenal, non-enhancing high-attenuation lesions >3 cm	Requires follow-up
III	Thickened smooth or irregular walls and/or septa in which measurable enhancement is present	50% malignant Intervention required as neoplasm cannot be excluded
IV	Distinct enhancing soft tissue components independent of the wall or septa. Also have features of category III lesions	Resection Clearly malignant

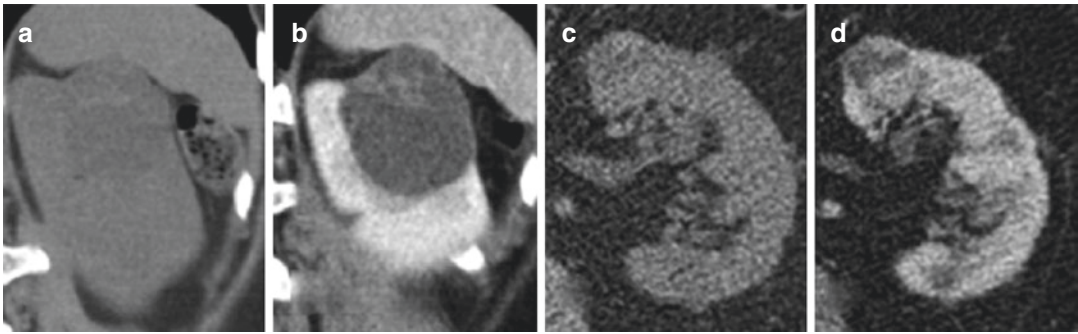


Fig. 3.13 Pre- (a) and (b) post-contrast coronal images of a left upper pole lesion with enhancing, irregular septa consistent with a Bosniak III lesion. Pre- (c) and (d) post-

contrast axial images of a Bosniak IV cystic left renal lesion containing an enhancing soft tissue nodule

sion index that quantifies tumour depth invasion into renal parenchyma [35] and renal pelvic score that assesses renal pelvis anatomy irrespective of renal tumour features [36].

Research has already begun evaluating these scoring systems to help risk-stratify patients undergoing partial nephrectomy (PN) and investigating whether these scores can predict surgical and oncological outcomes. Studies have shown that patients with higher scores have increased intraoperative complications [37, 38] and post-operative complications [39]. However, these studies have included predominately open PN and some laparoscopic PN series with more varied outcomes reported following robotic-assisted PN [40]. Higher morphometric scores have also been associated with increased risk of metastases and death from RCC, but further studies are needed to validate these relationships [41].

CT is the imaging workhorse in the evaluation of small renal masses. However, there are situations when MRI or ultrasound should be considered. Patients who cannot receive iodinated contrast media due to allergy or advanced kidney disease and individuals with genetic predisposition to renal tumours, who are likely to undergo serial imaging, should be offered alternate imaging modalities.

3.5 Magnetic Resonance Imaging (MRI)

MRI offers a reliable alternative to CT for the evaluation of small renal masses and is the imaging modality of choice in patients who are aller-

gic to iodinated contrast media. While MR contrast agents cannot be administered safely in end-stage renal failure, an unenhanced MRI is likely to yield better diagnostic information than unenhanced CT. MRI is also useful in patients who are likely to undergo serial imaging, to diminish the burden of ionizing radiation.

3.5.1 Protocol

MRI protocols used to evaluate renal masses vary depending on the manufacturer and institution. However, a generic renal mass protocol should include T2 fast spin echo (FSE) in three planes, axial T1 in and out of phase, fat-saturated 3D gradient-recalled echo (GRE) pre- and post-contrast (gadolinium) and diffusion-weighted imaging (DWI).

3.5.2 Enhancement

As with CT, the presence of enhancement following intravenous contrast is a key factor in distinguishing solid renal neoplasms from cysts. However, unlike CT, the tissue dose response to MRI contrast agents is non-linear, and consequently there is no universally accepted technique for measuring enhancement [8]. Described techniques include subjective, visual comparison [8, 42], image subtraction [8, 42–44] and quantitative increase in signal intensity [42, 44].

A quantitative increase in the signal intensity returned from a renal mass on post-gadolinium

T1-weighted images, of greater than 15%, is considered to represent enhancement. This 15% threshold for signal intensity increase will yield a 100% sensitivity for renal tumour and result in a lower than 6% false positive rate [46]. Subtraction imaging involves digital subtracting unenhanced T1-weighted images from an identical sequence performed post-contrast administration. This technique has a reported 99% sensitivity for solid renal tumours [44]. There is evidence the superior contrast resolution of MRI may overcome the problem of CT pseudoenhancement, allowing more accurate characterisation of small renal masses [8, 42] (Fig. 3.14).

3.5.3 Soft Tissue Characterisation

MRI provides superior soft tissue contrast compared with CT, which confers a number of potential advantages when evaluating small renal masses.

Macroscopic fat, indicating AML, can be readily identified within small renal masses on conventional T1, T2 and fat-suppressed sequences. There is evidence to suggest MRI may have utility in differentiating fat-poor AMLs from fat-containing RCCs based on the T2 signal characteristics of

these lesions. Fat-poor AMLs are hypointense on T2-weighted images due to the smooth muscle content, whereas clear cell RCCs are hyperintense [11, 47]. However, the diagnosis of fat-poor AMLs cannot be confidently based on this feature alone, as papillary RCCs can also demonstrate hypointensity on T2-weighted sequences [48] (Fig. 3.15).

Standard MRI sequences have not been shown to offer any greater sensitivity than CT in distinguishing between RCC and oncocytoma. Beer et al. found that both MRI and CT classified all oncocytomas within their series as surgical lesions [49]. Hecht et al. also classified all oncocytomas evaluated with MRI as malignant lesions [44]. This reflects a long-standing challenge in renal imaging, where no definite imaging features have been identified to distinguish oncocytoma from RCC. More recently, DWI has shown promise in the differentiation of RCC from oncocytoma, with one large meta-analysis demonstrating a statistically significant difference between the diffusion characteristics of these lesions [50].

The superior soft tissue contrast of MRI affords better visualisation of cyst contents and septations. In calcified cystic lesions, enhancement

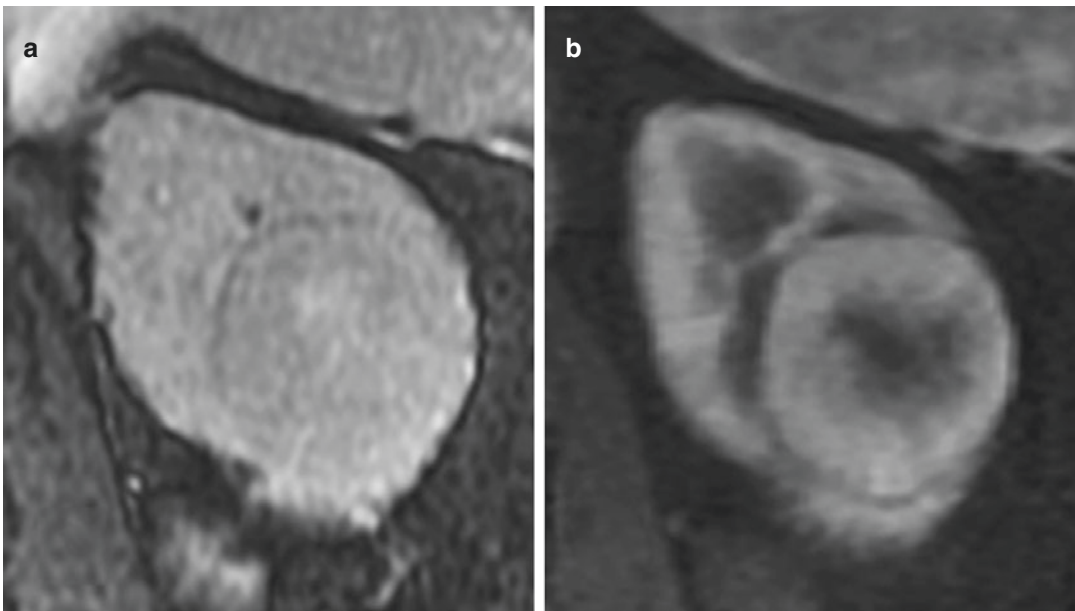


Fig. 3.14 Coronal T1-weighted (a) and post-contrast T1-weighted (b) images of a left lower pole renal mass demonstrating enhancement. Histology confirmed an RCC

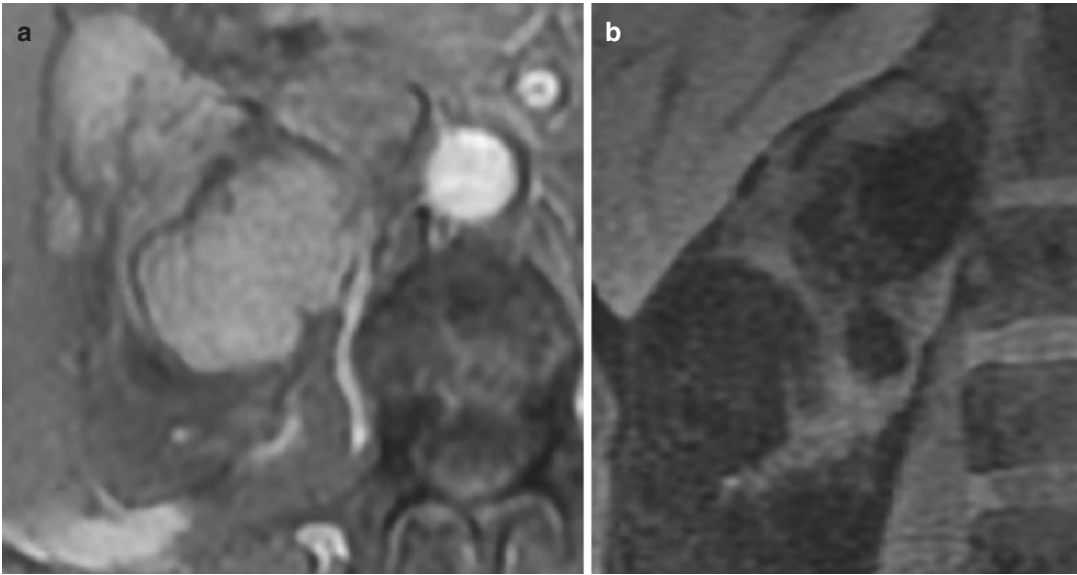


Fig. 3.15 Axial T1-weighted (a) and coronal fat-suppressed (b) sequences of an AML demonstrate macroscopic fat within the lesion

may also be better evaluated by MRI as, unlike CT, calcifications do not mask enhancement. In one study comparing MRI and CT evaluation of Bosniak cysts, MRI tended to upgrade the Bosniak category due to depiction of additional septa, improved visualisation of the cyst wall, septal thickening and enhancement. However, in this cohort of 69 renal masses, only two lesions were upgraded from non-surgical to surgical [7]. Beer et al. reported that of 56 lesions, none were upgraded from non-surgical to surgical lesions by MRI [49] (Fig. 3.16).

3.6 Ultrasound

Greyscale US is useful in distinguishing between solid and cystic renal masses; however, traditionally it has not played a further role in the evaluation of solid renal masses. With the advent of microbubble contrast agents, contrast-enhanced ultrasound (CEUS) has shown potential in the further evaluation of renal lesions. Microbubbles demonstrate tissue perfusion characteristics that are analogous to post-contrast enhancement seen with CT and MRI. Due to their size, microbubbles remain entirely intravascular which makes CEUS exquisitely sensitive to blood flow and can

demonstrate minimal flow not visible by CT. CEUS is increasingly utilised as a problem-solving tool in masses when enhancement is inadequately characterised by cross-sectional imaging. Microbubbles have an excellent safety profile [51] and can be used in patients with impaired renal function. The European Federation of Societies for Ultrasound in Medicine currently recommends CEUS for the characterisation of solid renal masses [52] (Fig. 3.17).

CEUS has also been used to evaluate solid renal lesions with encouraging results. Several small studies have examined the enhancement patterns of solid renal neoplasms, in particular comparing RCC and AMLs. Certain features including heterogeneous enhancement, enhanced peritumoural rim enhancement and early washout have been strongly associated with RCC [53–55].

CEUS is also proving of value in the assessment of cystic renal lesions. Several authors have compared CEUS with CT in the evaluation of cystic renal masses. Ascenti et al. found high concordance between CEUS and CECT in the characterisation of cystic lesions and 100% concordance between the modalities in categorising lesions as surgical or non-surgical [56]. Other studies support this, reporting CEUS to have a comparable diagnostic accuracy to CECT [57–59].

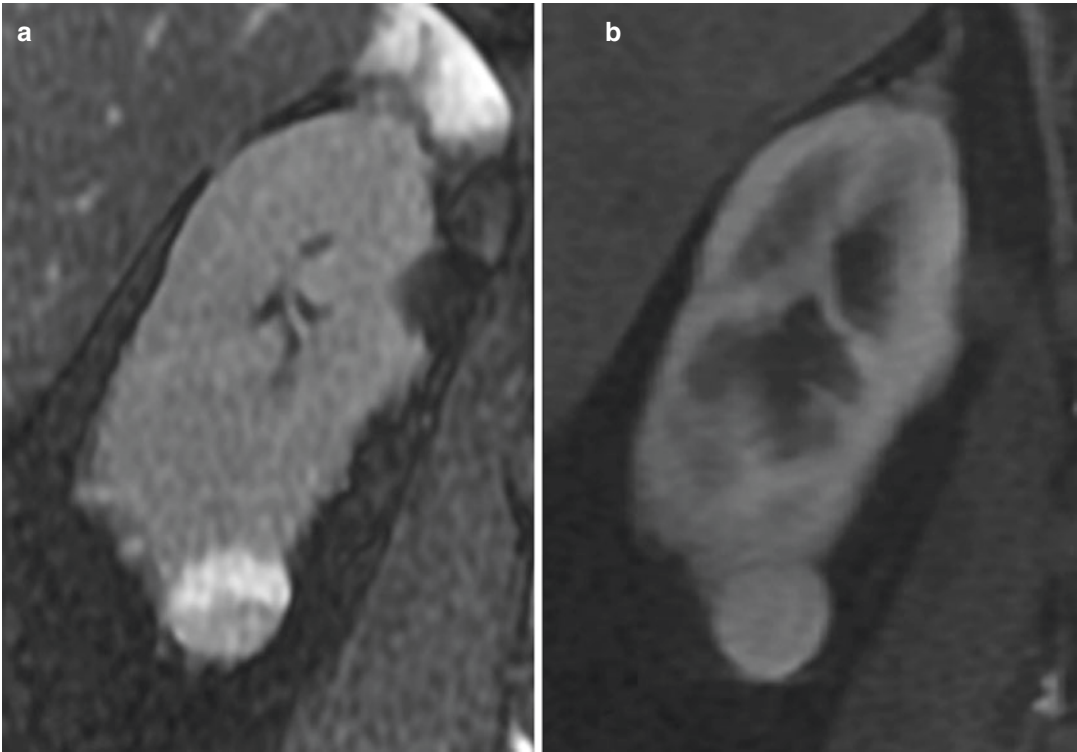


Fig. 3.16 Coronal T1-weighted MRI sequences pre- (a) and post-contrast (b) demonstrate no enhancement of the exophytic right lower pole lesion, consistent with a hyperdense cyst

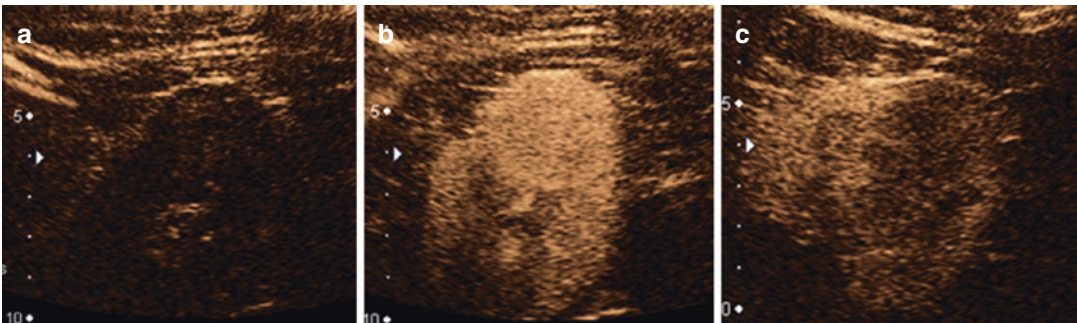


Fig. 3.17 CEUS showing typical enhancement pattern of a RCC. Figure (a) pre-contrast, with prompt enhancement in the early phase (b), and early washout (c). This lesion

demonstrated indeterminate enhancement on preceding CT. Histology confirmed a papillary RCC

3.7 Positron Emission Tomography

Fluorine-18 fluoro-2-deoxyglucose (FDG) positron emission tomography (PET) relies upon the cellular uptake of glucose to accumulate radio-

tracer within lesions in order to characterise them. Currently the role of FDG PET in small renal masses is limited for two key reasons. Firstly, normal renal parenchyma has high activity on FDG PET imaging tending to obscure small renal masses, and secondly FDG uptake is highly variable in RCC. Several studies have con-

firmed that PET has a more variable and overall poorer diagnostic accuracy in detecting RCC than CT [60–63]. Novel radiotracers may provide unique ways to characterise renal masses [64, 65], but these remain as research tools and have yet to find routine clinical application (Fig. 3.18).

3.8 Imaging-Guided Percutaneous Biopsy

Percutaneous biopsy of renal masses had largely fallen out of favour prior to the turn of the century, as the diagnostic accuracy of this procedure did not significantly outperform that of cross-sectional imaging. In a series of 2474 biopsies

reported by Lane et al., percutaneous biopsy only achieved a sensitivity and specificity of 70% and 60%, respectively, for the diagnosis of RCC [66]. With advances in imaging-guided percutaneous biopsy techniques and simultaneous developments in histological analysis, this technique now has an increasing role in the characterisation of small renal masses.

The benefits of obtaining a histological diagnosis are clear and include identifying surgical lesions from those found to be indeterminate on imaging, obtaining specific tumour subtype and grade information to help prognostication and guide systemic treatment and obtaining histological confirmation of malignancy prior to commencing ablative treatments such as radiofrequency ablation and cryotherapy.

Current imaging-guided biopsy techniques have sensitivities of 70–100% and specificity of 100% [66–74]. Small lesion size has been shown to negatively affect the diagnostic performance of percutaneous biopsy. Rybicki et al. reported lesions of 4–6 cm having greatest sensitivity and NPV of 97% and 89%, respectively, in comparison to 85% and 60% for lesions smaller than 3 cm [73]. Percutaneous biopsy has been shown to have a good safety profile with low rates of complications. Tumour seeding is only rarely encountered with only seven cases reported in the literature [75] (Fig. 3.19).

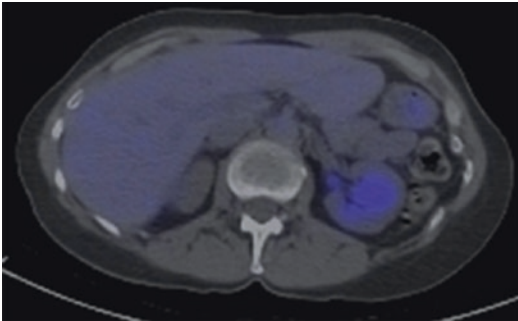


Fig. 3.18 Axial fused FDG PET-CT image demonstrating low-grade FDG avidity in the left kidney

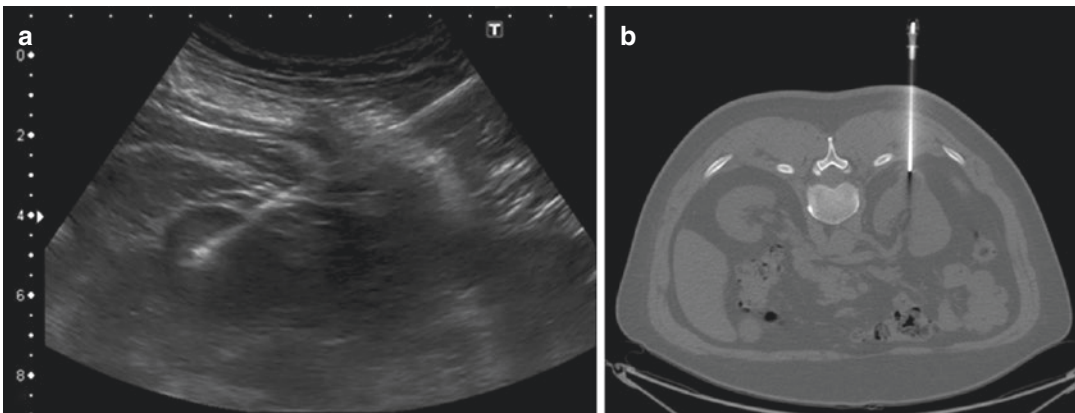


Fig. 3.19 Ultrasound-guided (a) and CT-guided (b) biopsy of a renal mass

Conclusions

Incidental detection of small renal masses on imaging, undertaken to evaluate unrelated symptoms or conditions, is a common occurrence. Subsequent management of small renal masses is dependent upon accurate imaging characterisation. Most small renal masses can be classified into surgical or non-surgical lesions by CT. However, in cases which are indeterminate by CT criteria, further investigation with MRI or CEUS will often lead to a definitive diagnosis. Considering the central role that imaging plays in the management of small renal masses, all clinicians involved in renal cancer treatment should have an understanding of the interpretation and diagnostic performance of the relevant imaging modalities.

References

1. Cancer Research UK. Kidney Cancer Statistics. <http://www.cancerresearchuk.org/health-professional/cancer-statistics/statistics-by-cancer-type/kidney-cancer#heading-Zero>. Accessed on 15 Nov 2014.
2. Jayson M, Sanders H. Increased incidence of serendipitously discovered renal cell carcinoma. *Urology*. 1998;51:203–5.
3. Cohen HT, McGovern FJ. Renal-cell carcinoma. *N Engl J Med*. 2005;353:2477–90.
4. Frank I, Blute ML, Chevillie JC, Lohse CM, Weaver AL, Zincke H. Solid renal tumours: an analysis of pathological features related to tumor size. *J Urol*. 2003;170:2217–20.
5. Kukitov A, Fossett LK, Ramchandani P, Tomaszewski JE, Siegelman ES, Banner MP, Van Arsdalen KN, Wein AJ, Malkowicz SB. Incidence of benign pathologic findings at partial nephrectomy for solitary renal mass presumed to be renal cell carcinoma on preoperative imaging. *Urology*. 2006;68:737–40.
6. Jeon HG, Lee SR, Kim KH, Oh YT, Cho NH, Rha KH, Yang SC, Han WK. Benign lesions after partial nephrectomy for presumed renal cell cancer in masses 4 cm or less: prevalence in Korean patients. *Urology*. 2010;76:574–9.
7. Israel GM, Hindman N, Bosniak MA. Evaluation of cystic renal masses: comparison of CT and MR imaging by using the Bosniak classification system. *Radiology*. 2004;231:365–71.
8. Israel GM, Bosniak MA. How I do it: evaluating renal masses. *Radiology*. 2005;236:441–50.
9. Maki DD, Birnbaum BA, Chakraborty DP, Jacobs JE, Carvalho BM, Herman GT. Renal cyst pseudoenhancement: beam hardening effects on CT numbers. *Radiology*. 1999;213:468–72.
10. Kim JK, Park SY, Shon JL, Cho KS. Angiomyolipoma with minimal fat: differentiation from renal cell carcinoma at biphasic helical CT. *Radiology*. 2004;230:677–84.
11. Jinzaki M, Tanimoto A, Narimatsu Y, Ohkuma K, Kurata T, Shinmoto H, Hiramatsu K, Mukai M, Murai M. Angiomyolipoma: imaging findings in lesions with minimal fat. *Radiology*. 1997;205:497–502.
12. Richmond L, Atri M, Sherman C, Sharir S. Renal cell carcinoma containing macroscopic fat on CT mimics an angiomyolipoma due to bone metaplasia without macroscopic calcification. *Br J Radiol*. 2010;83:179–81.
13. Strotzer M, Lehner KB, Becker K. Detection of fat in renal cell carcinoma mimicking angiomyolipoma. *Radiology*. 1993;188:427–8.
14. Prando A. Intratumoral fat in a renal cell carcinoma. *AJR Am J Roentgenol*. 1991;156:871.
15. Lesavre A, Correas J, Merran S, Grenier N, Vieillefond A, Helenon O. CT of papillary renal cell carcinomas with cholesterol necrosis mimicking angiomyolipomas. *AJR Am J Roentgenol*. 2003;181:143–5.
16. Chawla SN, Crispin PL, Hanlon AL, Greenberg RE, Chen DYT, Uzzo RG. The natural history of observed renal enhancing masses: meta-analysis and review of the world literature. *J Urol*. 2006;175:425–31.
17. Kassouf W, Aprikian AG, Laplante M, Tanguay S. Natural history of renal masses followed expectantly. *J Urol*. 2004;171:111–3.
18. Crispin PL, Viterbo R, Boorjian SA, Greenberg RE, Chen DYT, Uzzo RG. Natural history, growth kinetics, and outcomes of untreated clinically localized renal tumors under active surveillance. *Cancer*. 2009;115:2844–52.
19. Jewett MAS, Mattar K, Basiuk J, Morash CG, Pautler SE, Siemens DR, Tanguay S, Rendon RA, Gleave ME, Drachenberg DE, Chow R, Chung H, Chin JL, Fleshner NE, Evans AJ, Gallie BL, Haider MA, Kachura JR, Kurban G, Fernandes K, Finelli A. Active surveillance of small renal masses: progression patterns of early stage kidney cancer. *Eur Urol*. 2011;60:39–44.
20. Kunkle DA, Crispin PL, Chen DY, Greenberg RE, Uzzo RG. Enhancing renal masses with zero net growth during active surveillance. *J Urol*. 2007;177:849–53.
21. Siu W, Hafez KS, Johnston WK III, Wolf JS Jr. Growth rates of renal cell carcinoma and oncocytoma under surveillance are similar. *Urol Oncol*. 2007;25:115–9.
22. Smaldone MC, Kutikov A, Egleston BL, Canter DJ, Viterbo R, Chen DYT, Jewett MA, Greenberg RE, Uzzo RG. Small renal masses progressing to metastases under active surveillance. *Cancer*. 2012;118:997–1006.
23. Schatz SM, Lieber MM. Update on oncocytoma. *Curr Urol Rep*. 2003;4:30–5.

24. Quinn MJ, Hartman DS, Friedman AC, Sherman JL, Lautin EM, Pyatt RS, Ho CK, Csere R, Fromowitz FB. Renal oncocytoma: new observations. *Radiology*. 1984;153:49–53.
25. Choudharya S, Rajesha A, Mayerb NJ, Mulcahya KA, Haroon A. Renal oncocytoma: CT features cannot reliably distinguish oncocytoma from other renal neoplasms. *Clin Radiol*. 2009;64:517–22.
26. Siegel CL, McFarland EG, Brink JA, Fisher AJ, Humphrey P, Heiken JP. CT of cystic renal masses: analysis of diagnostic performance and interobserver variation. *AJR Am J Roentgenol*. 1997;169:813–8.
27. Parienty RA, Pradel J, Pariety I. Cystic renal cancers: CT characteristics. *Radiology*. 1985;157:741–4.
28. Bosniak MA. The current radiological approach to renal cysts. *Radiology*. 1986;158:1–10.
29. Curry NS, Cochran ST, Bissada NK. Cystic renal masses: accurate Bosniak classification requires adequate renal CT. *AJR Am J Roentgenol*. 2000;175:339–42.
30. Bosniak MA. Bosniak classification system for renal cysts and cystic tumours. *J Urol*. 1997;157:1852–3.
31. Warren KS, McFarlane J. The Bosniak classification of renal cystic masses. *BJU Int*. 2005;95:939–42.
32. Kutikov A, Uzzo RG. The R.E.N.A.L. nephrometry score: A comprehensive standardized system for quantitating renal tumor size, location and depth. *J Urol*. 2009;182:844–53.
33. Ficarra V, Novara G, Secco S, Macchi V, Porzionato A, De Caro R, Artibani W. Preoperative aspects and dimensions used for an anatomical (PADUA) classification of renal tumours in patients who are candidates for nephron-sparing surgery. *Eur Urol*. 2009;56:786–93.
34. Simmons MN, Ching CB, Samplaski MK, Park CH, Gill IS. Kidney tumor location measurement using the C index method. *J Urol*. 2010;183:1708–13.
35. Nisen H, Ruutu M, Glucker E, Visapaa H, Taari K. Renal tumour invasion index as a novel anatomical classification predicting urological complications after partial nephrectomy. *Scand J Urol*. 2014;48:41–51.
36. Tomaszewski JJ, Cung B, Smaldone MC, Mehrazin R, Kutikov A, Viterbo R, et al. Renal pelvic anatomy is associated with incidence grade and need for intervention for urine leak following partial nephrectomy. *Eur Urol*. 2013;pii: S0302.
37. Hayn MH, Schwaab T, Underwood W, Kim HL. RENAL nephrometry score predicts surgical outcomes of laparoscopic partial nephrectomy. *BJU Int*. 2011;108:87–1.
38. Khemees TA, Yuh BJ, Stacey A, Sharp DS, Abaza R, Box GN, et al. Post-operative morbidity of robotic versus open partial nephrectomy: the impact of preoperative tumour characteristics. *J Urol*. 2010;183:386.
39. Hew MN, Baseskioglu B, Barwari K, Axwijk PH, can C, Horenblas S, Bex a, de lat rosette JJMCH, Laguna pes MP. Critical appraisal of the PADUA classification and assessment of the RENAL nephrometry scores in patients undergoing partial nephrectomy. *J Urol*. 2011;186:42–6.
40. Millet I, Duyon FC, Pages E, Thuret R, Taourel P. Morphometric scores for renal tumours: what does the radiologist need to know? *Eur J Radiol*. 2014;83:1303–10.
41. Weight CJ, Atwell TD, Fassio RT, Kim SP, Kenny M, Lohse CM, et al. A multidisciplinary evaluation of inter-reviewer agreement of the nephrometry score and the prediction of long-term outcomes. *J Urol*. 2011;186:1223–8.
42. Willatt JM, Hussain HK, Chong S, Kappil M, Azar SF, Liu PS, Ruma JA, Elsayes KM. MR imaging in the characterisation of small renal masses. *Abdom Imaging*. 2014;39:761–9.
43. Pedrosa I, Sun MR, Spencer M, Genega EM, Olumi AF, Dewolf WC, Rofsky NM. MR imaging of renal masses: correlation with findings at surgery and pathologic analysis. *Radiographics*. 2008;28:985–1003.
44. Hecht EM, Israel GM, Krinsky GA, Hahn WY, Kim DC, Belitskaya-Levy I Lee VS. Renal masses: quantitative analysis of enhancement with signal intensity measurements versus qualitative analysis of enhancement with image subtraction for diagnosing malignancy at MR imaging. *Radiology*. 2004;232:373–8.
46. Ho VB, Allen SF, Hood MN, Choyke PL. Renal masses: quantitative assessment of enhancement with dynamic MR imaging. *Radiology*. 2002;224:695–700.
47. Hosokawa Y, Kinouchi T, Sawai Y, Mano M, Kiuchi H, Meguro N, Maeda O, Kuroda M, Usami M. Renal angiomyolipoma with minimal fat. *Int J Clin Oncol*. 2002;7:120–3.
48. Shinmoto H, Yuasa Y, Tanimoto A, Narimatsu Y, Jinzaki M, Hiramatsu K, Mukai M. Small renal cell carcinoma: MRI with pathologic correlation. *J Magn Reson Imaging*. 1998;8:690–4.
49. Beer AJ, Dobritz M, Zantl N, Weirich G, Stollfuss J, Rummeny EJ. Comparison of 16-MDCT and MRI for characterisation of kidney lesions. *AJR Am J Roentgenol*. 2006;186:1639–50.
50. Lassel EA, Rao R, Schwenke C, Schoenberg SO, Michaely HJ. Diffusion-weighted imaging of focal renal lesions: a meta-analysis. *Eur Radiol*. 2014;24:241–9.
51. Piscaglia F, Bolondi L. The safety of SonoVue in abdominal applications: retrospective analysis of 23188 investigations. *Ultrasound Med Biol*. 2006;32:1369–75.
52. Piscaglia F, Nolsoe C, Dietrich CF, Cosgrove DO, Gilja OH, et al. The EFSUMB guidelines and recommendations on the clinical practice of contrast enhanced ultrasound (CEUS): update 2011 on non-hepatic applications. *Ultraschall Med*. 2012;33:33–59.
53. Fan I, Lianfang D, Jinfang X, et al. Diagnostic efficacy of contrast-enhanced ultrasonography in solid renal parenchymal lesions with maximum diameters of 5cm. *J Ultrasound Med*. 2008;27:875–85.
54. Xu ZF, Xu HX, Xie XY et al. Renal cell carcinoma and renal angiomyolipoma: differential diagnosis with real-time contrast enhanced ultrasonography. *J Ultrasound Med* 2010; 29: 709–717.
55. Oh TH, Lee YH, Seo IY. Diagnostic efficacy of contrast-enhanced ultrasound for small renal masses. *Korean J Urol*. 2014;55:587–92.

56. Ascenti G, Mazziotti S, Zimbaro G, Settineri N, Magno C, Melloni D, Caruso R, Scribano E. Complex cystic renal masses: characterisation with contrast-enhanced ultrasound. *Radiology*. 2007;243:158–65.
57. Park BK, Kim B, Kim SH, Ko K, Lee HM, Choi HY. Assessment of cystic renal masses based on Bosniak classification: comparison of CT and contrast-enhanced US. *Eur J Radiol*. 2007;61:310–4.
58. Quaiá E, Bertolotto M, Cioffi V, Rossi A, Baratella E, Pizzolato R, Cova MA. Comparison of contrast-enhanced sonography and contrast-enhanced CT in the diagnosis of malignancy in complex cystic renal masses. *AJR Am J Roentgenol*. 2008;191:1239–49.
59. Ly X, Lu Q, Huang BJ, Ma JJ, Yan LX, Wen JX, Wang WP. Contrast-enhanced ultrasonography for evaluation of cystic renal mass: in comparison to contrast-enhanced CT and conventional ultrasound. *Abdominal Imaging*. 2014;39:1274–83.
60. Ramdave S, Thomas GW, Berlangieri S, et al. Clinical role of F-18 fluorodeoxyglucose positron emission tomography for detection and management of renal cell carcinoma. *J Urol*. 2001;166:825–30.
61. Kang DE, White RL Jr, Zuger JH, Sasser H, Teigland C. Clinical use of fluorodeoxyglucose F18 positron emission tomography for detection of renal cell carcinoma. *J Urol*. 2004;171:1806–9.
62. Ak I, Can C. F-18 FDG PET in detecting renal cell carcinoma. *Acta Radiol*. 2005;46:895–9.
63. Aide N, Cappele O, Bottet P, Bensadoun H, Regeasse A, Comoz F, Sobrio F, Bouvard G, Agostini. Efficiency of [18F] FDG PET in characterising renal cancer and detecting distant metastases: a comparison with CT. *Eur J Nucl Med Mol Imaging*. 2003;30:1236–45.
64. Divgi CR, Pandit-Taskar N, Jungbluth AA, Reuter VE, Gonen M, Ruan S, Pierre C, Nagel A, Pryma DA, Humm J, Larson SM, Old LJ, Russo P. Preoperative characterization of clear-cell renal carcinoma using iodine-124-labelled antibody chimeric G250 (124I-cG250) and PET in patients with renal masses: a phase 1 trial. *Lancet Oncol*. 2007;8:304–10.
65. Bolton DM, Wong P, Lawrentschuk N. Renal cell carcinoma: imaging and therapy. *Curr Opin Urol*. 2007;17:337–40.
66. Lane et al. Renal mass biopsy—a renaissance? *J Urol*. 2008;179:20–7.
67. Eshed I, Elias S, Sidi AA. Diagnostic value of CT guided biopsy of indeterminate renal masses. *Clin Radiol*. 2004;59:262–7.
68. Dechet CB, Zincke H, Sebo TJ, King BF, LeRoy AJ, Farrow GM, Blute ML. Prospective analysis of computerized tomography and needle biopsy with permanent sectioning to determine the nature of solid renal masses in adults. *J Urol*. 2003;169:71–4.
69. Richter F, Kasabian NG, Rj I Jr, Watson RA, Lang EK. Accuracy of diagnosis by guided biopsy of renal mass lesions classified indeterminate by imaging studies. *Urology*. 2000;55:348–52.
70. Hara I, Miyake H, Hara S, Arakawa S, Hanioka K, Kamidono S. Role of percutaneous image-guided biopsy in the evaluation of renal masses. *Urol Int*. 2001;67:199–202.
71. Lechevallier E, Andre M, Barriol D, et al. Fine needle percutaneous biopsy of renal masses with helical CT guidance. *Radiology*. 2000;216:506–10.
72. Caoili EM, Bude RO, Higgins EJ, Hoff DL, Nghiem HV. Evaluation of sonographically guided percutaneous core biopsy of renal masses. *AJR Am J Roentgenol*. 2002;179:373–8.
73. Rybicki FJ, Shu KM, Cibas ES, Fielding JR, van Sonnenberg E, Silverman SG. Percutaneous biopsy of renal masses: sensitivity and negative predictive value stratified by clinical setting and size of masses. *AJR Am J Roentgenol*. 2003;180:1281–73.
74. Sofikerim M, Tatlisen A, Canoz O, Tokat F, Demirtas A, Mavili E. What is the role of percutaneous needle core biopsy in diagnosis of renal masses? *Urology*. 2010;76:614–8.
75. Upport RN, Harisinghani MG, Gervais DA. Imaging-guided percutaneous renal biopsy: rationale and approach. *AJR Am J Roentgenol*. 2010;194:1443–9.